XLIII CILAMCE
21-25, November, 2022
FOZ DO IGUAÇU - PR - BRAZIL

Offshore wind farm layout optimization via metaheuristic algorithms using a three-dimensional analytical wake model

Anderson M. Ribeiro[1], Felipe S. Loureiro[2], Patrícia H. Hallak[3], Afonso C.C. Lemonge[3]

[1]*Graduate Program in Computational Modeling, Federal University of Juiz de Fora*
Jose Lourenço Kelmer St, São Pedro, Juiz de Fora, MG 36036-900, Brazil
andersonmr254@gmail.com
[2]*Dept. of Thermal and Fluid Sciences, Federal University of São João del-Rei*
Frei Orlando Sq, Center, São João del Rei - MG, 36307-352, Brazil
felipe.loureiro@ufsj.edu.br
[3]*Dept. of Applied and Computational Mechanics, School of Engineering, Federal University of Juiz de Fora*
Jose Lourenço Kelmer St, São Pedro, Juiz de Fora, MG 36036-900, Brazil
patricia.hallak@engenharia.ufjf.br, afonso.lemonge@ufjf.edu.br

Abstract. Due to the increasing demand for renewable energies, the wind energy industry has been in continuous progress through studies that aim to contribute to its technological advancement. This work proposes the minimization of the cost of energy (COE) of an offshore wind farm, given by the ratio between the cost of the farm and its annual energy production (AEP). For this purpose, the layout (continuous variables) and the different commercial types of each wind turbine (discrete variables) were considered as decision variables. Furthermore, econometric models were used to estimate the costs due to wind farm rated power, length of interconnection electricity cables between wind turbines, and different water depths to account for the supporting structures as a function of the installation layout for each wind turbine. To account for the mutual interference of the flow among the wind turbines and its impact on the AEP, and for comparison purposes, this study was conducted under two analytical wake models in the optimization process, namely, Gaussian wake model and the well-known Jensen wake model. The performance of the wind farm, subjected to different wind conditions, was then evaluated as a function of the probability of occurrence of wind direction and speed throughout the year to account for the AEP. To solve this optimization problem, the metaheuristics (Genetic Algorithm and Differential Evolution) were employed, resulting in a comparative study of their performance.

Keywords: Offshore wind farm, layout optimization, turbine selection, metaheuristics, cost of energy

1 Introduction

Due to the increasing demand for renewable energies, the advancement of the onshore and offshore wind industry has become increasingly necessary to meet the demands and solve the main challenges of the sector [1]. One of these challenges is the wake interaction between wind turbines, which are positioned close together due to reduced cabling costs, easier construction and maintenance, and reduced land requirements [2]. With the growth of offshore wind farms, the cost due to offshore structures, as well as the wind turbine cost and cabling cost, plays an important role in the whole wind farm design [3, 4]. The most applied approach in wind farm layout optimization (WFLO) is the usage of optimization metaheuristics, and since the classic work by Mosetti et al. [5], which applied the genetic algorithm with binary encoding and the Jensen wake model [6] on solving WFLO, many other metaheuristics and wind farm performance evaluation approaches have been applied on this topic [7, 8]. This paper proposes the minimization of the cost of energy (COE) of an offshore wind farm accounting for the layout and the different commercial types of each wind turbine selection. Computational experiments are performed considering different wind conditions, commercial wind turbines, wind farm performance assessment approaches and optimization metaheuristics. The remainder of this paper is organized as follows: Section 2 describes the main wind farm performance assessment approach adopted. Section 3 provides the cost assessment model used, which accounts for wind turbine, cabling and offshore supporting structures costs. The formulation of the WFLO problem and presentation of optimization metaheuristics applied are conducted in Section 4. Section 5 presents the numerical experiments and the analysis of their results. The paper ends with the conclusions reported in Section 6.

2 Wind farm performance

In the present work, the performance of the wind farm is evaluated through the annual energy production (AEP), calculated according to Gonzalez-Rodriguez et al. [9] by eq. (1):

$$AEP = T \sum_{i=1}^{N_t} \int_{u_{cut-in}}^{u_{cut-out}} \int_{0^\circ}^{360^\circ} P_{c_i}(\nu_i(u,\theta)) f(u,\theta)\, d\theta \ du \ , \tag{1}$$

where T is the total annual operation time of the wind farm; N_t is the number of installed wind turbines; u_{cut-in} and $u_{cut-out}$ are the cut-in and cut-out wind speed, respectively; P_{c_i} is the power curve of wind turbine i; ν_i is the effective wind speed at wind turbine i; u and θ are the atmospheric freestream wind speed (at a reference height H) and wind direction, respectively. In addition, $f(u,\theta)$ is the probability density function of occurrence of the pair (u,θ) throughout the year. The evaluation of ν_i was performed using the analytical Gaussian wake model proposed by Bastankhah and Porté-Agel [10] and shown in eq. (2).

$$\frac{u_\infty - u_{wake}}{u_\infty} = \left(1 - \sqrt{\frac{C_t}{8(k^* x/d_0 + \epsilon)^2}}\right) \times exp\left(-\frac{1}{2(k^* x/d_0 + \epsilon)^2}\left\{\left(\frac{z - z_h}{d_0}\right)^2 - \left(\frac{y}{d_0}\right)^2\right\}\right), \tag{2}$$

where C_t, d_0 and z_h are the thrust coefficient, the rotor diameter, and the hub height, respectively; u_∞ is the vertical wind speed profile in the atmospheric boundary layer and u_{wake} is the wake speed in a position (x,y,z), where x is the downwind location along the wind direction, y is the perpendicular distance to the wind direction and $z = 0$ on the ground; k^* is the wake growth rate; ϵ is the linear coefficient of the linear wake region expansion assumption proposed by Bastankhah and Porté-Agel [10] and its value is obtained through the relation $\epsilon = 0.25\left(0.5 \times \left(1 + \sqrt{1 - C_t}\right)/\sqrt{1 - C_t}\right)^{0.5}$ [10]. Niayifar and Porté-Agel [11] have proposed a relationship for k^* as a function of turbulence intensity I, given by: $k^* = 0.3837I + 0.003678$. The total turbulence intensity is obtained by $I^2 = I_0^2 + I_{wake}^2$ [12], where I_0 is the atmospheric turbulence intensity and I_{wake} the turbulence intensity added by the wake, calculated as Crespo and Hernández [12] by eq. (3).

$$I_{wake} = \begin{cases} 0.362\left(1 - \sqrt{1 - C_t}\right), & x < 3d_0 \\ 0.73\left(\frac{1 - \sqrt{1 - C_t}}{2}\right)^{0.83} I_0^{-0.0325}\left(\frac{x}{d_0}\right)^{-0.32}, & x \geq 3d_0 \ . \end{cases} \tag{3}$$

It was considered neutral atmospheric stability for the atmospheric freestream velocity and turbulence intensity profile [13, 14], making it possible to use the logarithmic profile [15]. The wake superposition model by Niayifar and Porté-Agel [11], shown in eq. (4), was applied to resolve the wake superposition of the N_t wind turbines within the wind farm, and thus evaluate ν_i in each wind turbine i as follows:

$$\nu_i = u_\infty - \sum_{k=1}^{N_M} (u_k - u_{ki}) \ , \tag{4}$$

where N_M is the number of wind turbines upstream of the wind turbine i; u_k is the effective velocity in each upstream wind turbine k and u_{ki} represents the wake speed of the wind turbine k wake evaluated in position (x_i, y_i, z_i) of wind turbine i. Because this is an analytical model, ν_i was evaluated only in positions of interest, in order to reduce computational cost. Therefore the wake speed was evaluated at 9 points of interest for each wind turbine, as shown in Fig. 1a [2], and ν_i is evaluated as an average of these values in each wind turbine. The performance of each wind turbine i is evaluated according to its power curve $P_{c_i}(\nu_i)$, given by eq. (5):

$$P_{c_i}(\nu_i) = \begin{cases} 0, & \nu_i \leq u_{cut-in} \\ f_{power_i}(\nu_i), & u_{cut-in} < \nu_i \leq u_{Rated_i} \\ P_{Rated_i}, & u_{Rated_i} < \nu_i \leq u_{cut_out} \\ 0, & \nu_i > u_{cut-out} \ , \end{cases} \tag{5}$$

where $f_{power_i}(\nu_i)$ is an interpolation function created by the points provided by the manufacturer for the power curve of each wind turbine, P_{Rated_i} is its rated power and u_{Rated_i} is the wind speed at which P_{Rated_i} is reached. Fig. 1b shows the power curves of the different wind turbine models considered in this work, obtained from TheWindPower.net [16].

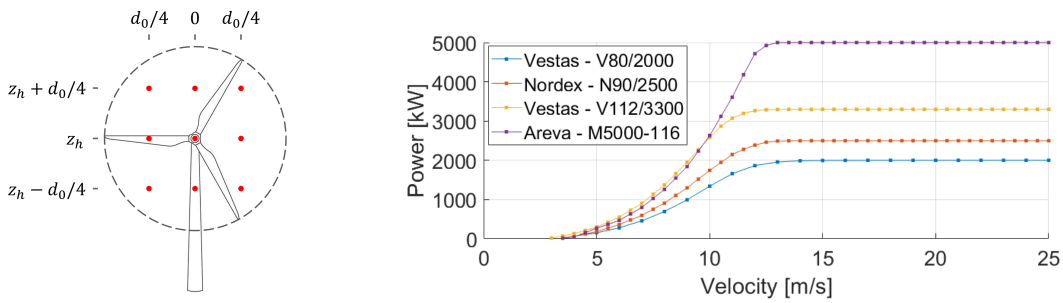

(a) Points of interest for evaluating ν_i

(b) Power curves $P_{c_i}(\nu_i)$

Figure 1. Performance of the wind turbines

In order to estimate the AEP of the wind farm for different values of u and θ, which leads to different wind farm performance throughout the year, it was taken into consideration the probability density function $f(u, \theta)$ in such a way that $\int_{u_{cut-in}}^{u_{cut-out}} \int_{0^\circ}^{360^\circ} f(u, \theta)\, d\theta \; du \; = 1$ [17, 18].

3 Cost Model

To account for the wind farm cost, defined here as $Cost_{WF} = Cost_{WT} + Cost_{Cables} + Cost_{Sup.structures}$, the wind turbine cost was taken into account ($Cost_{WT}$), as well as the cost due to total length of the electrical interconnection cables ($Cost_{Cables}$) and the cost of the wind turbine supporting structures ($Cost_{Sup.structures}$). The portion of the cost due to the wind turbines and the cable length are given by eq. (6) and eq. (7) [4], respectively.

$$Cost_{WT} = 1374 \times \left(\sum_{i=1}^{N_t} P_{Rated_i} \right)^{0.87}, \tag{6}$$

$$\begin{aligned} Cost_{Cables} = \big[& (4.26 \times 10^{-4} \times A + 2.324 \times 10^{-1}) + \\ & (-2.2684 \times 10^{-3} \times N_t + 3.8018 \times 10^{-1}) \big] \times L_c, \end{aligned} \tag{7}$$

where L_c is the total length of the cables and A is its cross sectional area. It was adopted an average value of $A = 260\, mm^2$ among the values presented by Gonzalez-Rodriguez [4]. L_c is calculated according to the distance $\Delta_{ij} = \sqrt{(x_i - x_j)^2 + (y_i - y_j)^2} \,|\, j \neq i$ and $i, j \in [1, N_t]$ between a given wind turbine i and all the other wind turbines j. For each wind turbine i, a portion of the total length is added corresponding to the average distance between the three wind turbines j adjacent to it, i.e., those three wind turbines j with smaller Δ_{ij} values. The cost $Cost_{Sup.structures}$ is related to a water depth (WD) function, which models water depth until the seabed as a function of the coordinates (x, y). In this way, the WD function evaluated at each wind turbine i position returns the water depth for each installation position, i.e., $WD_i(x_i, y_i)$. Eq. (8) considers the cost of the supporting structures of each wind turbine i as a function of WD_i and P_{Rated_i} [4].

$$Cost_{Sup.structures} = \sum_{i=1}^{N_t} \left(0.9181 \times WD_i^2 - 31.433 \times WD_i + 747.4 \right) \times P_{Rated_i}. \tag{8}$$

4 Formulation of the optimization problem and evolutionary algorithms

The optimization problem solved in this work is posed as eq. (9):

$$\begin{aligned} \min \quad COE(\mathbf{x}) = & \quad \frac{Cost_{WF}(\mathbf{x})}{AEP(\mathbf{x})}, \\ \text{subject to :} & \quad \sum_{i=1}^{N_t} \sum_{\substack{j=1 \\ j \neq i}}^{N_t} \frac{\psi_{ij}}{d_{min}} \leq 0 \\ & \quad \mathbf{x}_L \leq \mathbf{x} \leq \mathbf{x}_U, \end{aligned} \tag{9}$$

where $COE(\mathbf{x})$ is the cost of energy, d_{min} is the minimum distance allowed between a wind turbine i and another wind turbine j, usually of 5 times a reference rotor diameter [19] and $\psi_{ij} = d_{min} - \Delta_{ij} \iff d_{min} - \Delta_{ij} \geq 0$ and $d_{min} - \Delta_{ij} < 0 \implies \psi_{ij} = 0$. It can be stated that this constraint will also hinder wind turbines of being allocated in positions which violate the applicability of eq. (2) model, i.e., for downwind distance $x/d_o \leq 3$ [10]. The design variables vector is $\mathbf{x} = \{x_1, y_1, mod_1, ..., x_i, y_i, mod_i, ..., x_{N_t}, y_{N_t}, mod_{N_t}\}^T$, in which x_i and y_i are continuous and represent the installation coordinate (x_i, y_i) for each wind turbine i, while mod_i is discrete and represents the wind turbine i model, among those pre-established in Fig. 1b. The lower $\mathbf{x}_L$ and upper $\mathbf{x}_U$ bounds for the decision variables are defined as $-L/2 \leq x_i \leq L/2$, $-H/2 \leq y_i \leq H/2$ and $1 \leq mod_i \leq N_{WT_{types}}$, where L and H are the wind farm dimensions and $N_{WT_{types}}$ is the number of pre-established wind turbines.

To solve the optimization problem given by eq. (9), the PlatEMO platform was used [20] employing the metaheuristics Genetic Algorithm (GA) and Differential Evolution (DE). Concerning the DE, in addition to the classic mutation strategy implemented in PlatEMO (DE/rand/1), it was also included the DE/current to best/1 mutation strategy [21]. For such a purpose, a change was carried out in the original PlatEMO.

5 Numerical experiments

A total of 20 independent runs of the algorithms used in each of the cases specified in Table 1 was conducted. In all cases $N_t = 10$ wind turbines were considered, whereby Vestas-V80/2000, Nordex-N90/2500, Vestas-V112/3300 and Areva-M5000-116 imply mod_i equals to 1, 2, 3 and 4, respectively. The used water depth function, in meters, was $WD(x, y) = -0.002 \times \sqrt{(x-2500)^2 + (y-2500)^2} - 30$ and $WD(x, y) = -30 \; \forall (x, y) \,|\, (x-2500)^2 + (y-2500)^2 \leq 1000^2$. In the present work, a more simplified wind distribution case was used, considering a single wind speed of $u = 8$ m/s (at a reference height $H = 70$ m) and occurring in only 4 directions ($0°, 45°, 90°$ and $135°$) with equal probability of occurrence each in $f(u, \theta)$. The population size was also held constant for all cases ($N = 200$), the maximum number of evaluations of the objective function ($MaxFE = 1.5 \times 10^5$) and for $\mathbf{x}_L$ and $\mathbf{x}_U$ the values of $L = H = 12$ km and $N_{WT_{types}} = 4$ were considered.

In addition to the Gaussian wake model of eq. (2), this work also addresses the widely used Jensen wake model [6–8] as well as the wake superposition model [5, 6] for evaluating ν_i, as means of comparison between both wake models. Unlike for the Gaussian wake model, in which ν_i was evaluated as discribed in Fig. 1a, for the Jensen model the position of interest is only the coordinate (x_i, y_i, z_i) of each wind turbine i, being z_i its hub height, since the effect of intersection between wake area and rotor area is already accounted as described in Kunakote et al. [7].

Table 1. Numerical Experiments

Cases	Algorithm	Algorithm Parameters [20]	Wake Model
C1	DE/Current to best/1	$CR = 0.9$; $F = 0.5$	Gaussian
C2	DE/Current to best/1		Jensen
C3	DE/Rand/1		Gaussian
C4	DE/Rand/1		Jensen
C5	GA	$proC = proM = 1$; $disC = disM = 20$	Gaussian
C6	GA		Jensen

Table 2 shows a summary of the results for each case in Table 1. It can be seen that GA had a better performance among all algorithms. It also noticed that the performance of the mutation strategy DE/current to best/1 outperforms the classic strategy DE/rand/1 in this study case. Fig. 2 shows the evolution of the objective function (eq. (9)) over the evaluations for each case. It can be seen that the mutation strategy DE/rand/1 had difficulties in converging within the $MaxFE$ allowable evaluations, in both wake models (C3 and C4), being worse than DE/current to best/1. So the strategy DE/current to best/1 will be used in the following comparisons with GA.

In all cases the choice of model for each wind turbine converged to model 3, as expected, given the only wind speed that occurs in the wind farm 8 m/s and, by analyzing the Fig. 1b and eq. (6), it can be observed that the model 3 wind turbine has the highest conversion capacity at the lowest cost for this wind speed. The only exception was case C3, which pointed out one of the wind turbines with model 2.

Fig. 3 shows the layouts proposed for each case. It can be observed that for all of them, the positioning of the wind turbines tended towards the region with lower water depths, in order to reduce the costs of the supporting structures. Fig. 4 and Fig. 5 show, for the Gaussian and Jensen wake models respectively, the wind speed fields at the hub height of the wind turbines (z_h) and the wind farm layout efficiency η_{WF}, measured by means of ν_i at each wind turbine i and the freestream wind speed at hub height u_{z_h} for each wind direction θ along the N_θ directions considered in the optimization, as $\eta_{WF} = \left(\sum_{n=1}^{N_\theta} \sum_{i=1}^{N_t} \nu_i(\theta_n)\right) / (N_t \times N_\theta \times u_{z_h})$.

Table 2. Summary of results for each case (C.), where f_{min} means the best result, f_{max} the worst, f_{mean} the average and σ_f means the standart deviation.

C.	f_{min}	f_{max}	f_{mean}	σ_f	C.	f_{min}	f_{max}	f_{mean}	σ_f	C.	f_{min}	f_{max}	f_{mean}	σ_f
C1	1.179	1.231	1.204	0.015	C3	1.288	1.333	1.308	0.014	C5	1.172	1.185	1.176	0.004
C2	1.155	1.185	1.168	0.008	C4	1.240	1.295	1.273	0.013	C6	1.144	1.161	1.149	0.004

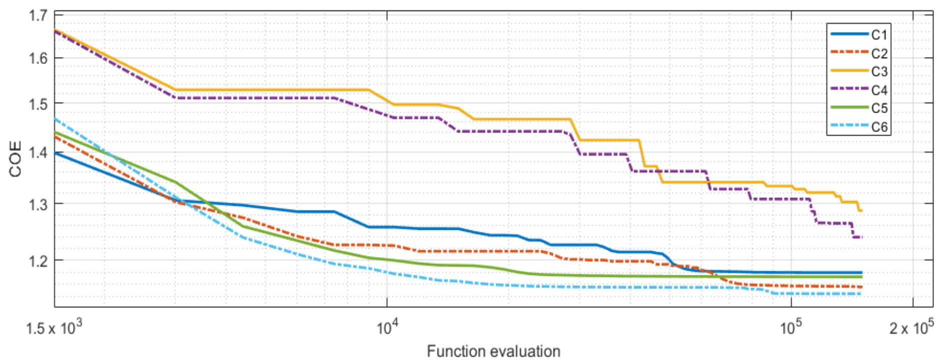

Figure 2. Cost of energy vs. function evaluation acordding to each case

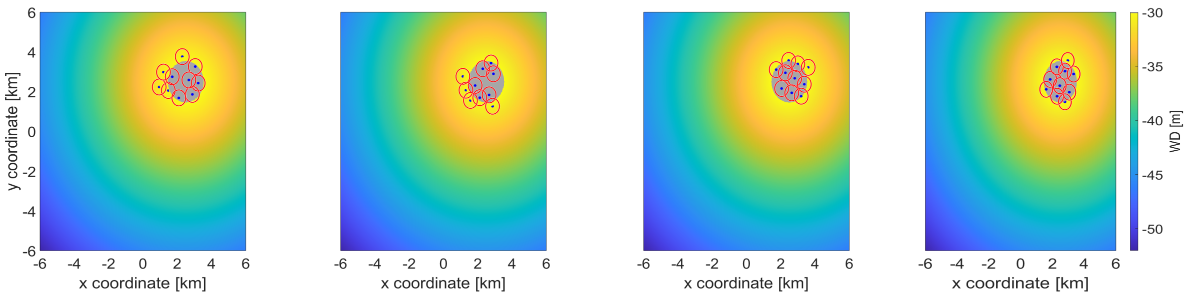

(a) $C1$ (b) $C2$ (c) $C5$ (d) $C6$

Figure 3. Comparison of layouts for cases C1, C2, C5 and C6

Although the result of case C6 presented the lowest value of COE, equal to 1.144, when the layout proposed by this case is evaluated according to the Gaussian wake model, the cost of energy becomes COE = 1.335, i.e.,

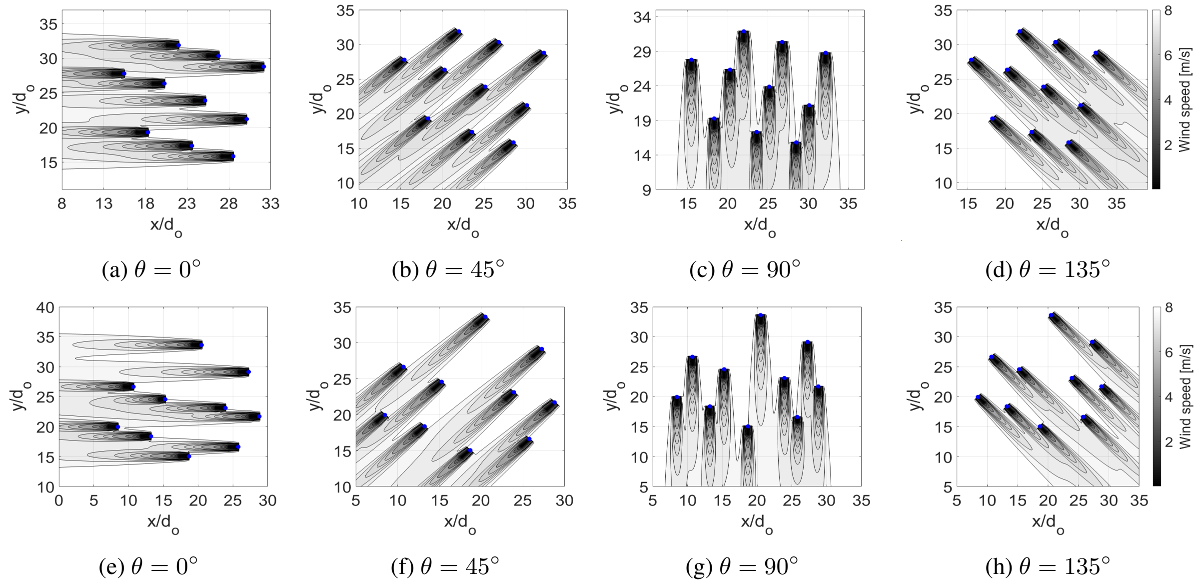

(a) $\theta = 0°$ (b) $\theta = 45°$ (c) $\theta = 90°$ (d) $\theta = 135°$

(e) $\theta = 0°$ (f) $\theta = 45°$ (g) $\theta = 90°$ (h) $\theta = 135°$

Figure 4. Wind speed field of the best run with GA: (a)-(d) $(\eta_{WF} = 99.5896\,\%)$ and with DE: (e)-(h) $(\eta_{WF} = 99.6787\,\%)$ using Gaussian wake model.

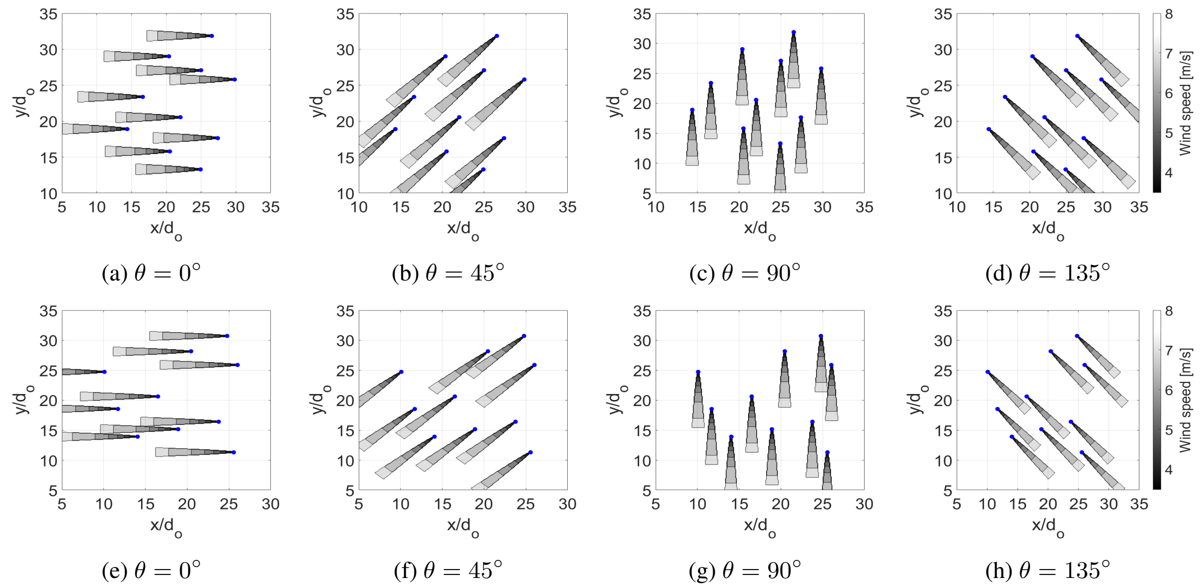

(a) $\theta = 0°$ (b) $\theta = 45°$ (c) $\theta = 90°$ (d) $\theta = 135°$

(e) $\theta = 0°$ (f) $\theta = 45°$ (g) $\theta = 90°$ (h) $\theta = 135°$

Figure 5. Wind speed field of the best run with GA: (a)-(d) $(\eta_{WF} = 100.00\,\%)$ and with DE: (e)-(h) $(\eta_{WF} = 100.00\,\%)$ using Jensen wake model.

larger than the one obtained by case C5. This is due to the Jensen model underestimating the velocity deficit $(u_\infty - u_{wake})/u_\infty$ [10].

6 Conclusions

Through the comparison performed between the both wake models, it is concluded that although the Jensen model is faster than the Gaussian model, the Jensen model leads to layouts underestimating the velocity deficits, i.e., the wake effects among the wind turbines. The comparison between the different mutation strategies for the DE showed that the DE/current to best/1 strategy outperforms the classical DE/rand/1 for this case study, however GA showed slightly superior results.

Acknowledgements. The authors thank the Graduate Program in Computational Modeling (PPGMC/UFJF), Federal University of Juiz de Fora (UFJF), Federal University of São João del-Rei (UFSJ) and Brazilian Agency FAPEMIG for the financial support.

Authorship statement. The authors hereby confirm that they are the sole liable persons responsible for the authorship of this work, and that all material that has been herein included as part of the present paper is either the property (and authorship) of the authors, or has the permission of the owners to be included here.

References

[1] van G. A. M. Kuik, J. Peinke, R. Nijssen, D. Lekou, J. Mann, J. N. Sørensen, C. Ferreira, J. W. van Wingerden, D. Schlipf, P. Gebraad, H. Polinder, A. Abrahamsen, G. J. W. van Bussel, J. D. Sørensen, P. Tavner, C. L. Bottasso, M. Muskulus, D. Matha, H. J. Lindeboom, S. Degraer, O. Kramer, S. Lehnhoff, M. Sonnenschein, P. E. Sørensen, R. W. Künneke, P. E. Morthorst, and K. Skytte. Long-term research challenges in wind energy - a research agenda by the european academy of wind energy. *Wind Energy Science*, vol. 1, n. 1, pp. 1–39, 2016.

[2] A. P. J. Stanley, O. Roberts, J. King, and C. J. Bay. Objective and algorithm considerations when optimizing the number and placement of turbines in a wind power plant. *Wind Energy Science*, vol. 6, n. 5, pp. 1143–1167, 2021.

[3] IRENA. *Renewable Power Generation Costs in 2020*. International Renewable Energy Agency, Abu Dhabi, 2021.

[4] A. G. Gonzalez-Rodriguez. Review of offshore wind farm cost components. *Energy for Sustainable Development*, vol. 37, pp. 10–19, 2017.

[5] G. Mosetti, C. Poloni, and B. Diviacco. Optimization of wind turbine positioning in large windfarms by means of a genetic algorithm. *Journal of Wind Engineering and Industrial Aerodynamics*, vol. 51, n. 1, pp. 105–116, 1994.

[6] I. Katic, J. Højstrup, and N. O. Jensen. A simple model for cluster efficiency. In *European wind energy association conference and exhibition*, volume 1, pp. 407–410. A. Raguzzi Rome, Italy, 1986.

[7] T. Kunakote, N. Sabangban, S. Kumar, G. Tejani, N. Panagant, N. Pholdee, S. Bureerat, and A. Yildiz. Comparative performance of twelve metaheuristics for wind farm layout optimisation. *Archives of Computational Methods in Engineering*, vol. 29, 2021.

[8] J. F. Herbert Acero, O. Probst, P.-E. Réthoré, G. Larsen, and K. Castillo-Villar. A review of methodological approaches for the design and optimization of wind farms. *Energies*, vol. Energies, pp. 6930–7016, 2014.

[9] A. G. Gonzalez-Rodriguez, J. Serrano-González, M. Burgos-Payán, and J. M. Riquelme-Santos. Realistic optimization of parallelogram-shaped offshore wind farms considering continuously distributed wind resources. *Energies*, vol. 14, n. 10, 2021.

[10] M. Bastankhah and F. Porté-Agel. A new analytical model for wind-turbine wakes. *Renewable Energy*, vol. 70, pp. 116–123. Special issue on aerodynamics of offshore wind energy systems and wakes, 2014.

[11] A. Niayifar and F. Porté-Agel. Analytical modeling of wind farms: A new approach for power prediction. *Energies*, vol. 9, n. 9, 2016.

[12] A. Crespo and J. Hernández. Turbulence characteristics in wind-turbine wakes. *Journal of Wind Engineering and Industrial Aerodynamics*, vol. 61, n. 1, pp. 71–85, 1996.

[13] L. F. de Assis Tavares, M. Shadman, L. P. de Freitas Assad, C. Silva, L. Landau, and S. F. Estefen. Assessment of the offshore wind technical potential for the brazilian southeast and south regions. *Energy*, vol. 196, pp. 117097, 2020.

[14] F. M. Pimenta, A. R. Silva, A. T. Assireu, V. d. S. e. Almeida, and O. R. Saavedra. Brazil offshore wind resources and atmospheric surface layer stability. *Energies*, vol. 12, n. 21, 2019.

[15] S. Emeis. Current issues in wind energy meteorology. *Meteorological Applications*, vol. 21, 2014.

[16] TheWindPower.net. The wind power - wind energy market inteligence. `https://www.thewindpower.net/index.php`, accessed 27 Jun 2022.

[17] J. Manwell, J. McGowan, and A. Rogers. *Wind Energy Explained: Theory, Design and Application*. Wiley, 2010.

[18] J. Feng and W. Z. Shen. Modelling wind for wind farm layout optimization using joint distribution of wind speed and wind direction. *Energies*, vol. 8, n. 4, pp. 3075–3092, 2015.

[19] P. Lissaman, G. Gyatt, and A. Zalay. Critical issues in the design and assessment of wind turbine arrays. In *Int. Symp. Wind Energy Syst., Proc.;(United Kingdom)*, volume 2, 1982.

[20] Y. Tian, R. Cheng, X. Zhang, and Y. Jin. PlatEMO: A MATLAB platform for evolutionary multi-objective optimization. *IEEE Computational Intelligence Magazine*, vol. 12, n. 4, pp. 73–87, 2017.

[21] S. Das, S. S. Mullick, and P. Suganthan. Recent advances in differential evolution – an updated survey. *Swarm and Evolutionary Computation*, vol. 27, pp. 1–30, 2016.